Micro Nano Bio Aspects

https://www.mnba-journal.com

Online ISSN: 2980-8081

Docking of the main protein receptors of SARS-CoV-2 by hesperidin metabolite: In silico study

Qassim Hassan Aubais Aljelehawy

Department of Chemistry, College of Education, University of Al-Qadisiyah, Iraq

ARTICLE INFO

Original paper

Article history:
Received: 28 July 2023
Revised: 19 Aug 2023
Accepted: 20 Aug 2023
ePublished: 22 Aug 2023

Keywords:
CB-Dock, Binding energy, Virulence factors, SARS-CoV-2 helicase, Viral replication

ABSTRACT

Identifying and designing novel antiviral agents are indispensable affairs in biomedicine. Hesperidin is a flavonoid that is commonly present as a secondary metabolite of citrus fruits. Severe acute respiratory syndrome coronavirus 2 (SARS-CoV-2) outbreaks have caused a main threat to human health owing to its highly contagious nature. Previous studies showed antiviral activities of this bioactive compound against several virulence factors of SARS-CoV-2. The helicase of SARS-CoV-2 is essential for viral replication. In the present study, we evaluated the docking of hesperidin with helicase, RNA-dependent RNA polymerase (RdRp), papain-like protease (PL^{pro}), and main proteases (M^{pro}) of SARS-CoV-2 by CB-Dock as a protein-ligand docking method. This secondary metabolite had a low binding energy (-9.6 kcal/mol) toward the SARS-CoV-2 helicase. This study showed that hesperidin may be considered a more desirable therapeutic agent for future investigations.

DOI: https://doi.org/10.22034/mnba.2023.409047.1040

Introduction

Biocompatibility, biodegradability, and therapeutic properties of polyphenols including flavonoids, ellagitannin, and tannic acid have been reported by various investigations [1, 2]. Hesperidin as a flavonoid has obtained attention in experimental and computational methods, specifically docking investigations [3]. The major therapeutic properties of hesperidin including antifungal, antibacterial, antiviral, and anticancer activities may be found in both micro and nanoformulations [4-7]. The low bioavailability of hesperidin by about 20% is the major limitation for effective clinical application of this metabolite [8]. Finding new promising antivirals is the crucial affair, particularly against life-threatening viruses [9, 10]. In this regard, drug repurposing or drug repositioning approaches can be used to discover novel therapeutic agents from the existing approved drug molecules based on Food and Drug Administration (FDA) [11]. Moreover, identifying new effective strategies according to natural compounds is the great issue.

Severe acute respiratory syndrome coronavirus-2 (SARS-CoV-2) caused the global pandemic, named coronavirus disease 2019 (COVID-19) [10]. Molecular docking studies have illustrated that hesperidin can bind to multiple receptors of SARS-CoV-2 including proteases (main proteases (M^{pro}) and papain-like protease (PL^{pro}) modulating the host's innate immune response), spike protein, and angiotensin-converting enzyme 2 (ACE2) [12]. SARS-CoV-2 replication is regulated by RNA-dependent RNA polymerase (RdRp) and helicase [13]. In this study, interactions of hesperidin metabolite with M^{pro}, helicase, PL^{pro}, and RdRp of SARS-CoV-2 have been surveyed by the CB-Dock server.

Materials and methods

Ligand was hesperidin prepared from the PubChem database (**Figure 1a**). Viral targets including helicase (PDB code: 6ZSL, resolution: 1.94 Å), RdRp (PDB code: 6M71, resolution: 2.90 Å), PL^{pro} (PDB code: 3E9S, resolution: 2.50 Å), and M^{pro} (PDB code: 6LU7,

*Corresponding author. E-mail: qassim.hassan@qu.edu.iq

resolution: 2.16 Å) have been obtained from protein data bank (PDB) (**Figures 1b-e**). The UCSF Chimera1.12 program was employed to minimization of the compounds. A molecular docking study was performed by the CB-Dock server (http://clab.labshare.cn/cb-dock/php/index.php) [14, 15].

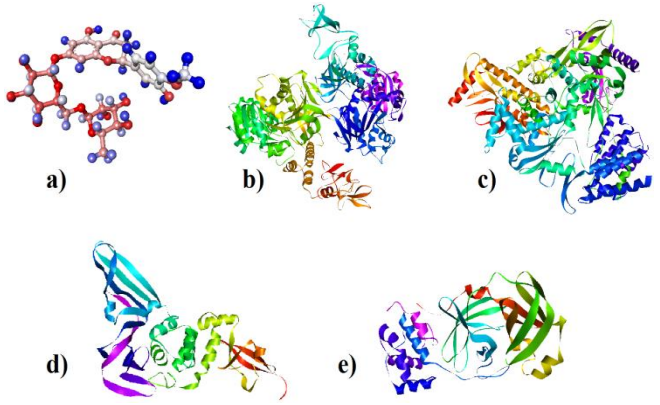

Fig. 1. Chemical and molecular structures of hesperidin (a), helicase (b), RdRp (c), PL^{pro} (d), and M^{pro} (e).

Results and discussion

CB-dock results demonstrated that hesperidin can dock PL^{pro}, M^{pro}, RdRp, and helicase by best Vina scores of −8.1, −8.6, −9, and −9.6 kcal/mol towards cavity volumes of 243, 258, 775, and 2984 $Å^3$, respectively (Tables 1-4). Highest affinity was indicated for hesperidin-helicase with Vina score of -9.6 kcal/mol and interacting amino acids of ASN177, ARG178, ASN179, LEU405, PRO406, ALA407, PRO408, ARG409, LEU412, THR413, LYS414, GLY415, THR416, LEU417, PHE422, SER485, SER486, PRO514, TYR515, ASN516, THR532, ASP534, SER535, HIS554, ASN557, and ARG560 related to chain B (Table 4). The docking interaction of hesperidin with the SARS-CoV-2 NSP13 helicase with related H-bonds have been illustrated in Figure 2. Previous docking study via CB-Dock displayed Vina scores of −8.3 and −9.9 kcal/mol for quercetin and epigallocatechin gallate against spike glycoprotein (S-glycoprotein) of SARS-CoV-2 [16]. In a similar study, theaflavin digallate, biorobin, hesperidin, rosmarinic acid, and berchemol exhibited binding energy values of −10.574, −9.058, −7.848, −6.971, and −6.793 kcal/mol toward M^{pro}, respectively [17]. Among the 14 terpenoids, best binding energies of −8.40 , −8.35, −8.79, and −8.51 kcal/mol were respectively identified for ichangin ($C_{26}H_{32}O_9$), deacetylnomilin ($C_{28}H_{34}O_9$), β-amyrin ($C_{30}H_{50}O$), and nomilin ($C_{28}H_{34}O_9$) toward M^{pro} [18]. In a comparative study, the binding energy and interaction of 76 drugs against RdRp and M^{pro} of SARS-CoV-2 were evaluated by GOLD 5.7 (Genetic Optimisation for Ligand Docking) and AutoDock Vina. Based on this study, raltegravir, daclatasvir, simeprevir, cobicistat, and remdesivir exhibited −9.7, −9.5, −9.3, −8.4, and −7.2 kcal/mol binding energies, respectively against RdRp model protein. Three main bonds including hydrophobic, electrostatic, and hydrogen bonds have been indicated for these docking interactions [19]. The docking interaction of glycyrrhizin bioactive compound related to licorice root was compared to chloroquine, hydroxychloroquine, remdesivir, GS-441524, and arbidol drugs against M^{pro} enzyme. The glycyrrhizin and remdesivir showed the highest negative free energy values of − 8.21 and − 7.12 kcal/ mole, respectively. Interestingly, these energy values were approximately similar to the best-docked pose of O6K ligand as a reference with $\Delta G = -7.40$ kcal/mol [20]. Other antiviral drugs including ACV triphosphate, BVDUTP, adefovir, tenofovir, HPmpa, and stavudine displayed respectively, binding energies of −8.04, −7.50, −7.23, −6.82, −6.72, and −6.27 kcal/mol toward site 2 in the wild spike protein. In the case of site 1 in the wild spike protein, cytarabine, brivudine, PMEG diphosphate, rilpivirine, inosine, and stavudine drugs showed docking scores of −8.92, −8.86, −8.46, −7.87, −7.64, and −7.57, respectively [21]. Secondary metabolites of apigenin, ellagic acid, chlorogenic acid, myricetin, chrysin, and quercetin related to *Moringa oleifera* plant species demonstrated −6.5, −7.1, −6.6, −6.1, −6.8, and −6.6 kcal/mol if binding energy, respectively in interaction with non-structural protein 9 (Nsp9) [22]. This protein contributes to viral replication of SARS-CoV-2 during the infection of human cells [23]. Natural and synthetic peptides may be used as suitable candidates for inactivation of viruses, particularly SARS-CoV-2 [24, 25]. There were −744.8, −703, −700.8, and −814.4 kJ/mol for the interaction of synthetic peptides including RcAlb-PepII, RcAlb-PepIII, Mo-CBP3-PepIII, and Mo-CBP3-PepII with SARS-CoV2 spike protein in the open state, respectively [26].

Table 1. CB-dock results for hesperidin-3E9S.

CurPocket ID	Vina score (kcal/mol)	Cavity volume (Å^3)	Center (x, y, z)	Docking size (x, y, z)	Contact residues
C3	-8.1	243	-5, 26, 15	24, 24, 24	**Chain A**: PRO34 TYR36 LEU59 PRO60 SER61 ASP62 ARG66 SER67 ALA69 PHE70 THR75 LEU76 ASP77 GLU78 SER79 PHE80 LEU81 GLY82 ARG83
C2	-7.7	647	-28, 21, 28	24, 24, 24	**Chain A**: GLY164 ASP165 VAL166 ARG167 MET209 ALA247 PRO248 PRO249 TYR265 GLY267 ASN268 TYR269 GLN270 CYS271 GLY272 TYR274 PRO300 THR302 ASP303
C1	-7.5	712	-8, 12, 9	24, 24, 24	**Chain A**: ASP13 ASN14 ASP38 GLY39 PHE57 TYR72 TYR73 TYR84 MET85 LEU88 LYS92 ALA132 GLU135 ALA136 ARG139 ASP144 ALA146 ASN147 LEU151
C5	-7.3	203	-40, 11, 10	24, 24, 24	**Chain A**: GLN98 GLY101 LEU102 THR103 LEU121 GLN122 GLN123 LEU124 GLU125 VAL126 TYR137 ALA140 ARG141 ALA142 PHE259 LEU260 CYS261 THR278 ALA279 LYS280 LYS307
C4	-6.3	212	-28, 8, 27	24, 24, 24	**Chain A**: TRP107 ASN110 THR266 GLY267 CYS271 GLY272 HIS273 THR275 ARG285 ASP287 HIS290

Table 2. CB-dock results for hesperidin-M^{pro}.

CurPocket ID	Vina score (kcal/mol)	Cavity volume (Å^3)	Center (x, y, z)	Docking size (x, y, z)	Contact residues
C3	-8.6	258	-14, 11, 72	24, 24, 24	**Chain A**: THR24 THR25 THR26 LEU27 HIS41 VAL42 CYS44 MET49 TYR54 PHE140 LEU141 ASN142 GLY143 SER144 CYS145 HIS163 HIS164 MET165 GLU166 LEU167 PRO168 HIS172 PHE181 VAL186 ASP187 ARG188 GLN189 THR190 ALA191 GLN192
C1	-8.1	688	-24, 1, 56	24, 24, 24	**Chain A**: ARG131 LYS137 ASP197 THR198 THR199 VAL204 TYR237 ASN238 TYR239 LEU271 LEU272 LEU286 LEU287 GLU288 ASP289 GLU290
C5	-7.7	212	-34, 16, 54	24, 24, 24	**Chain A**: PHE8 VAL104 ARG105 ILE106 GLN107 PRO108 GLN110 THR111 PHE112 ASN151 ASP153 SER158 VAL202 HIS246 ILE249 PRO293 PHE294 VAL297

C2	-7.4	548	-14, 34, 56	24, 24, 24	**Chain A**: GLU14 GLY15 CYS16 MET17 GLN19 TRP31 GLN69 ALA70 GLY71 ASN72 VAL73 ASN95 PRO96 LYS97 ASN119 GLY120 SER121 PRO122
C4	-6.9	239	-37, 5, 58	24, 24, 24	**Chain A**: ARG105 ILE106 GLN107 PRO108 GLY109 GLN110 THR111 PRO132 ASN151 ILE200 VAL202 ASN203 GLU240 ASP245 HIS246 ILE249 THR292 PRO293

Table 2 (continued).

Table 3. CB-dock results for hesperidin-RdRp.

CurPocket ID	**Vina score (kcal/mol)**	**Cavity volume ($Å^3$)**	**Center (x, y, z)**	**Docking size (x, y, z)**	**Contact residues**
C2	-9.0	775	127, 135, 127	24, 24, 24	**Chain A**: SER255 TYR265 ILE266 LYS267 TRP268 LEU270 SER318 THR319 VAL320 PHE321 PRO322 PRO323 THR324 PHE326 ARG349 LEU388 LEU389 ASP390 THR393 THR394 CYS395 PHE396 SER397 PRO461 **Chain B**: LEU122 TYR149
C3	-7.8	724	120, 120, 136	24, 24, 24	**Chain A**: ASP452 LYS545 ARG553 ALA554 ARG555 THR556 VAL557 TRP617 ASP618 TYR619 PRO620 LYS621 CYS622 ASP623 ARG624 THR680 SER682 THR687 ASN691 SER759 ASP760 ASP761
C1	-7.7	1089	122, 139, 100	24, 24, 24	**Chain A**: VAL231 PRO232 VAL233 VAL234 ASP235 TYR289 TRP290 ASP291 GLN292 ASP303 ARG305 CYS306 ARG467 LEU470 TYR732 ARG733 ASN734 ARG735 ASP736
C4	-6.4	574	146, 132, 82	24, 24, 24	**Chain A**: PHE35 LYS50 LYS73 ARG74 THR76 ASN79 GLU83 ILE114 ARG116 VAL204 THR206 ASP208 ASN209 ASP218 PHE219 GLY220 ASP221 PHE222
C5	-6.1	549	121, 96, 146	24, 24, 24	**Chain A**: PHE429 LYS430 GLU431 GLY432 GLU436 LEU437 LYS438 PHE440 **Chain C**: LYS2 MET3 SER4 LYS7 LYS43 ASP44 THR45

Table 4. CB-dock results for hesperidin-helicase.

CurPocket ID	Vina score (kcal/ mol)	Cavity volume ($Å^3$)	Center (x, y, z)	Docking size (x, y, z)	Contact residues
C3	-9.6	2984	-23, 20, -21	35, 24, 30	**Chain B**: ASN177 ARG178 ASN179 LEU405 PRO406 ALA407 PRO408 ARG409 LEU412 THR413 LYS414 GLY415 THR416 LEU417 PHE422 SER485 SER486 PRO514 TYR515 ASN516 THR532 ASP534 SER535 HIS554 ASN557 ARG560
C1	-9.1	4329	-32, 20, -49	24, 24, 30	**Chain B**: VAL193 GLN194 ILE195 GLY196 GLU197 THR214 THR215 TYR217 ALA336 VAL340 GLU341 **Chain A**: PHE182 THR183 TYR185 GLN194 ILE195 GLY196 GLU197 THR215 THR228 ALA336 ARG337
C4	-8.9	2136	-16, 35, -64	24, 24, 24	**Chain A**: LEU138 LYS139 GLU142 GLU143 PHE145 LYS146 TYR149 ASN179 TYR180 VAL181 GLU197 LEU227 THR228 ALA308 CYS309 SER310 ARG339 VAL360 ASN361 MET378 THR380 ASP383 ALA407 PRO408 ARG409 THR410
C2	-8.6	3723	-11, 20, -69	24, 32, 35	**Chain A**: LYS139 GLU142 GLU143 LYS146 ASN179 TYR180 VAL181 GLU197 LEU227 THR228 HIS230 THR231 VAL232 MET233 CYS309 ASN361 MET378 THR380 TYR382 ASP383 VAL386 ARG390 ALA407 PRO408 ARG409 THR410
C5	-8.5	2002	-32, 29, -75	30, 24, 24	**Chain A**: PHE145 TYR149 ARG173 PRO175 LEU176 ASN177 ASN179 TYR180 PRO408 ARG409 THR410 LEU411 LEU412 THR413 ASP483 VAL484 SER485 SER486 ALA487 PRO514 TYR515 ASN516 SER517 THR532 ASP534 SER535 HIS554 ARG560

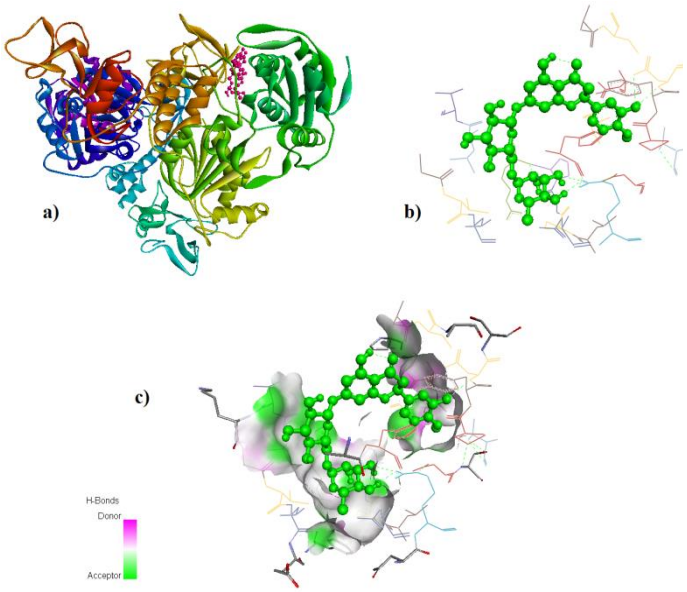

Fig. 2. Docking site for model 3 of CB-Dock (a), interaction of amino acids related to the viral helicase with hesperidin (b), and the surface around hesperidin ligand (c).

Conclusions

Molecular docking studies can improve the designing and finding of novel therapeutic agents cost-effectively. Hesperidin had a lower binding energy toward the SARS-CoV-2 helicase compared to RdRp, PL^{pro}, and M^{pro} of SARS-CoV-2. This study showed that hesperidin may be considered a more desirable therapeutic agent for inhibiting viral replication. This docking study presented an insight into molecular interaction to understand the antiviral mechanism and the spatial orientation of the hesperidin ligand that can be used for drug design. More studies are needed to evaluate other flavonoids against virulence factors of SARS-CoV-2. In addition, ameliorating the low bioavailability of hesperidin should be considered in future studies.

Abbreviations

ACE2: Angiotensin-converting enzyme 2
COVID-19: Coronavirus disease 2019
FDA: Food and drug administration
GOLD: Genetic optimisation for ligand docking
M^{pro}: Main proteases
PL^{pro}: Papain-like protease
RdRp: RNA-dependent RNA polymerase
SARS-CoV-2: Severe acute respiratory syndrome coronavirus 2
S-glycoprotein: Spike glycoprotein

Study Highlights

- Molecular docking studies can improve the designing and finding of novel therapeutic agents cost-effectively.
- Hesperidin had a lower binding energy toward the SARS-CoV-2 helicase compared to RdRp, PL^{pro}, and M^{pro} of SARS-CoV-2.
- More studies are needed to evaluate other flavonoids against virulence factors of SARS-CoV-2.

Funding

This work was not supported by any institutes.

Conflict of interest

Not applicable.

Ethical approval

This article does not contain any studies with animals or human participants performed by any of the authors.

Author contributions

Not applicable.

Acknowledgments

Declared none.

References

1. Ahmadi S, Javid H. Novel formulations of ellagic acid for the improvement of antimicrobial, antioxidant, anticancer, antidiabetic, and neuroprotective applications. Nano Micro Biosystems. 2023;2(1):31-5. doi:https://doi.org/10.22034/nmbj.2023.388479.1015
2. Adefegha SA, Salawi A, Bumrungpert A, Khorasani S, Torkaman S, Mozafari MR, et al. Encapsulation of polyphenolic compounds for health promotion and disease prevention: Challenges and opportunities. Nano Micro Biosystems. 2022;1(2):1-12. doi:https://doi.org/10.22034/nmbj.2023.163756
3. Bahador A, Vaezi M. Novel formulations of hesperidin for antitumor, antimicrobial, and neuroprotective effects: A review. Micro Nano Bio Aspects. 2023:-. doi:https://doi.org/10.22034/mnba.2023.394932.1030
4. Liu Y, Benohoud M, Galani Yamdeu JH, Gong YY, Orfila C. Green extraction of polyphenols from citrus peel by-products and their antifungal activity against Aspergillus flavus. Food Chemistry: X. 2021;12:100144. doi:https://doi.org/10.1016/j.fochx.2021.100144
5. Zhao Z-y, Li P-j, Xie R-s, Cao X-y, Su D-l, Shan Y.

Biosynthesis of silver nanoparticle composites based on hesperidin and pectin and their synergistic antibacterial mechanism. International Journal of Biological Macromolecules. 2022;214:220-9. doi:https://doi.org/10.1016/j.ijbiomac.2022.06.048
6. Attia GH, Moemen YS, Youns M, Ibrahim AM, Abdou R, El Raey MA. Antiviral zinc oxide nanoparticles mediated by hesperidin and in silico comparison study between antiviral phenolics as anti-SARS-CoV-2. Colloids and Surfaces B: Biointerfaces. 2021;203:111724.
doi:https://doi.org/10.1016/j.colsurfb.2021.111724
7. Pandey P, Khan F. A mechanistic review of the anticancer potential of hesperidin, a natural flavonoid from citrus fruits. Nutrition Research. 2021;92:21-31. doi:https://doi.org/10.1016/j.nutres.2021.05.011
8. Wdowiak K, Walkowiak J, Pietrzak R, Bazan-Woźniak A, Cielecka-Piontek J. Bioavailability of Hesperidin and Its Aglycone Hesperetin-Compounds Found in Citrus Fruits as a Parameter Conditioning the Pro-Health Potential (Neuroprotective and Antidiabetic Activity)-Mini-Review. Nutrients. 2022;14(13). doi:https://doi.org/10.3390/nu14132647
9. Baeshen MN, Attar R, Bouback TA, Albeshri AO, Baeshen NN, Karkashan A, et al. Assaying for antiviral activity of the folkloric medicinal desert plant Rhazya stricta on coronavirus SARS-CoV-2. Biotechnology & Biotechnological Equipment. 2022;36(1):68-74. doi:https://doi.org/10.1080/13102818.2022.2047107
10. Aljelehawy Q, Mal Allah OR, Sourazur G. Physicochemical properties, medicinal chemistry, toxicity, and absorption of quercetin and its interaction with spike glycoprotein of SARS-CoV-2: Molecular docking. Nano Micro Biosystems. 2022;1(1):32-9. doi:https://doi.org/10.22034/nmbj.2022.163207
11. Sahoo BM, Ravi Kumar BVV, Sruti J, Mahapatra MK, Banik BK, Borah P. Drug Repurposing Strategy (DRS): Emerging Approach to Identify Potential Therapeutics for Treatment of Novel Coronavirus Infection. Frontiers in Molecular Biosciences. 2021;8. doi:https://doi.org/10.3389/fmolb.2021.628144
12. Agrawal PK, Agrawal C, Blunden G. Pharmacological Significance of Hesperidin and Hesperetin, Two Citrus Flavonoids, as Promising Antiviral Compounds for Prophylaxis Against and Combating COVID-19. Natural Product Communications. 2021;16(10):1934578X211042540. doi:https://doi.org/10.1177/1934578x211042540
13. Wang Y, Anirudhan V, Du R, Cui Q, Rong L. RNA-dependent RNA polymerase of SARS-CoV-2 as a therapeutic target. Journal of Medical Virology. 2021;93(1):300-10.
doi:https://doi.org/10.1002/jmv.26264
14. Cao Y, Li L. Improved protein–ligand binding affinity prediction by using a curvature-dependent surface-area model. Bioinformatics. 2014;30(12):1674-80. doi:https://doi.org/10.1093/bioinformatics/btu104
15. Liu Y, Grimm M, Dai W-t, Hou M-c, Xiao Z-X, Cao Y. CB-Dock: a web server for cavity detection-guided protein–ligand blind docking. Acta Pharmacologica Sinica. 2020;41(1):138-44. doi:https://doi.org/10.1038/s41401-019-0228-6
16. Alavi M, Mozafari MR, Ghaemi S, Ashengroph M, Hasanzadeh Davarani F, Mohammadabadi M. Interaction of Epigallocatechin Gallate and Quercetin with Spike Glycoprotein (S-Glycoprotein) of SARS-CoV-2: In Silico Study. Biomedicines. 2022;10(12):3074.
doi:https://doi.org/10.3390/biomedicines10123074
17. Peele KA, Potla Durthi C, Srihansa T, Krupanidhi S, Ayyagari VS, Babu DJ, et al. Molecular docking and dynamic simulations for antiviral compounds against SARS-CoV-2: A computational study. Informatics in Medicine Unlocked. 2020;19:100345. doi:https://doi.org/10.1016/j.imu.2020.100345
18. Giofrè SV, Napoli E, Iraci N, Speciale A, Cimino F, Muscarà C, et al. Interaction of selected terpenoids with two SARS-CoV-2 key therapeutic targets: An in silico study through molecular docking and dynamics simulations. Computers in Biology and Medicine. 2021;134:104538.
doi:https://doi.org/10.1016/j.compbiomed.2021.104538
19. Ahmed S, Mahtarin R, Ahmed SS, Akter S, Islam MS, Mamun AA, et al. Investigating the binding affinity, interaction, and structure-activity-relationship of 76 prescription antiviral drugs targeting RdRp and Mpro of SARS-CoV-2. Journal of Biomolecular Structure and Dynamics. 2021;39(16):6290-305. doi:https://doi.org/10.1080/07391102.2020.1796804
20. Rai H, Barik A, Singh YP, Suresh A, Singh L, Singh G, et al. Molecular docking, binding mode analysis, molecular dynamics, and prediction of ADMET/toxicity properties of selective potential antiviral agents against SARS-CoV-2 main protease: an effort toward drug repurposing to combat COVID-19. Molecular Diversity. 2021;25(3):1905-27. doi:https://doi.org/10.1007/s11030-021-10188-5
21. Poustforoosh A, Hashemipour H, Tüzün B, Azadpour M, Faramarz S, Pardakhty A, et al. The Impact of D614G Mutation of SARS-COV-2 on the Efficacy of Anti-viral Drugs: A Comparative Molecular Docking and Molecular Dynamics Study. Current Microbiology. 2022;79(8):241. doi:https://doi.org/10.1007/s00284-022-02921-6
22. Muhammad S, Hassan SH, Al-Sehemi AG, Shakir HA, Khan M, Irfan M, et al. Exploring the new potential antiviral constituents of Moringa oliefera for SARS-COV-2 pathogenesis: An in silico molecular docking and dynamic studies. Chemical Physics Letters. 2021;767:138379.

doi:https://doi.org/10.1016/j.cplett.2021.138379
23. de O. Araújo J, Pinheiro S, Zamora WJ, Alves CN, Lameira J, Lima AH. Structural, energetic and lipophilic analysis of SARS-CoV-2 non-structural protein 9 (NSP9). Scientific Reports. 2021;11(1):23003. doi:https://doi.org/10.1038/s41598-021-02366-0
24. Schütz D, Ruiz-Blanco YB, Münch J, Kirchhoff F, Sanchez-Garcia E, Müller JA. Peptide and peptide-based inhibitors of SARS-CoV-2 entry. Adv Drug Deliv Rev. 2020;167:47-65. doi:https://doi.org/10.1016/j.addr.2020.11.007
25. Zannella C, Chianese A, Greco G, Santella B, Squillaci G, Monti A, et al. Design of Three Residues Peptides against SARS-CoV-2 Infection. Viruses. 2022;14(10):2103. doi:https://doi.org/10.3390/v14102103
26. Souza PFN, Lopes FES, Amaral JL, Freitas CDT, Oliveira JTA. A molecular docking study revealed that synthetic peptides induced conformational changes in the structure of SARS-CoV-2 spike glycoprotein, disrupting the interaction with human ACE2 receptor. International Journal of Biological Macromolecules. 2020;164:66-76. doi:https://doi.org/10.1016/j.ijbiomac.2020.07.174

HOW TO CITE THIS ARTICLE:
Aljelehawy QHA. Docking of the main protein receptors of SARS-CoV-2 by hesperidin metabolite: In silico study. Micro Nano Bio Aspects. 2023; 2(3): 24-31.
doi: https://doi.org/10.22034/mnba.2023.409047.1040